LOC554202 contributes to chordoma progression by sponging miR-377-3p and up-regulating SMAD3

Guang Xu*, Jingnan Liu*, Jun He, Haibo He, Xiaotao Su and Qianhuan Gui

Chordoma is a rare malignant bone tumor originating from the remnants of the notochord. Here, the role of long noncoding LOC554202 in chordoma progression and its associated mechanism were explored. Cell proliferation was analyzed by 3-(4, 5-dimethylthiazol-2-yl)-2, 5 diphenyltetrazolium bromide and colony formation assays. Flow cytometry was conducted to analyze cell apoptosis rate. The migration and invasion of chordoma cells were analyzed by transwell migration and invasion assays and wound healing assays. A xenograft tumor model was established in nude mice to explore the role of LOC554202 in regulating tumor growth *in vivo*. The interaction between microRNA-377-3p (miR-377-3p) and LOC554202 or sekelsky mothers against d PP (SMAD) family member 3 (SMAD3) was verified by dual-luciferase reporter and RNA immunoprecipitation assays. The glycolytic rate of chordoma cells was analyzed using glucose assay kit, lactic acid kit and ApoSENSOR ADP/ATP ratio assay kit. LOC554202 expression was upregulated in chordoma tissues and cell lines. LOC554202 silencing suppressed the proliferation, migration and invasion and induced the apoptosis of chordoma cells. LOC554202 knockdown restrained xenograft tumor growth *in vivo*. miR-377-3p was confirmed as a target of LOC554202, and miR-377-3p silencing largely overturned LOC554202 knockdown-mediated anti-tumor effects in chordoma cells. miR-377-3p interacted with the 3′ untranslated region (3′UTR) of SMAD3 and miR-377-3p overexpression-mediated antitumor effects in chordoma cells were largely attenuated by SMAD3 overexpression. LOC554202 could positively regulate SMAD3 expression by sponging miR-377-3p in chordoma cells. LOC554202 contributed to the glycolysis of chordoma cells by targeting binding to miR-377-3p/SMAD3 axis. LOC554202 facilitated the proliferation, migration, invasion and glycolysis and inhibited the apoptosis of chordoma cells by mediating miR-377-3p/SMAD3 axis. *Anti-Cancer Drugs* 34: 15–28

Anti-Cancer Drugs 2023, **34**:15–28

Keywords: chordoma, LOC554202, miR-377-3p, SMAD3

Department of Spinal Surgery, The Affiliated Nanhua Hospital, Hengyang Medical College, University of South China, Hengyang, Hunan, China

Correspondence to Qianhuan Gui, Department of Spinal Surgery, The Affiliated Nanhua Hospital, Hengyang Medical College, University of South China, 336 Dongfeng South Road, Zhuhui District, Hengyang, 421000, Hunan, China
Tel: +86 0734 835 8008; e-mail: nanhyy123@163.com

*Dr. Guang Xu and Dr. Jingnan Liu contributed equally to this work.

Received 8 March 2022 **Revised form accepted** 21 March 2022

Highlights

1. LOC554202 is upregulated in chordoma tissues and cell lines.
2. LOC554202 knockdown suppresses the proliferation, migration, invasion and glycolysis and induces the apoptosis of chordoma cells.
3. LOC554202/miR-377-3p/SMAD3 axis is established for the first time.
4. LOC554202 contributes to chordoma progression through mediating miR-377-3p/SMAD3 axis.

Introduction

Chordoma is a rare bone tumor that primarily attacks the sacrococcygeal and skull base regions in older male adults [1–3]. Chordoma is highly resistant to chemotherapy or radiotherapy, and surgical resection is the first choice for chordoma patients, followed by high-dose radiotherapy [4,5]. Nevertheless, local recurrence and metastasis are common in chordoma patients [6,7]. Therefore, understanding the molecular mechanism behind chordoma development is important to develop novel effective therapeutic strategies.

Long noncoding RNAs (lncRNAs) play important roles in human diseases, including tumorigenesis [8,9]. LOC554202 might exert diverse roles in different malignancies. For instance, Ding *et al.* [10] found that LOC554202 was downregulated in colorectal cancer, and it induced the apoptosis of colorectal cancer cells. Shi *et al.* [11] reported that LOC554202 expression was upregulated in breast cancer, and it contributed to breast cancer development. As for chordoma, Ma *et al.* [12] found that LOC554202 facilitated the proliferation, migration and invasion of chordoma cells by regulating EZH2 and microRNA-31 (miR-31). However, the working mechanism of LOC554202 in chordoma progression is not fully addressed.

Supplemental Digital Content is available for this article. Direct URL citations appear in the printed text and are provided in the HTML and PDF versions of this article on the journal's website, www.anti-cancerdrugs.com.

0959-4973 Copyright © 2022 The Author(s). Published by Wolters Kluwer Health, Inc. DOI: 10.1097/CAD.0000000000001327

Accumulating evidence have suggested that microRNAs (miRNAs) are implicated in tumorigenesis and development [13,14]. Through bioinformatics analysis, miR-377-3p was predicted as a candidate target of LOC554202 in this study. Previous studies identified miR-377-3p as a tumor suppressor in many malignancies [15–19]. Huang *et al*. [15] found that miR-377-3p restrained colorectal cancer progression by regulating XIAP, zinc finger E-box-binding homeobox 2 and wingless/integrated/β-catenin signaling. Xie *et al*. [19] found that lncRNA small nucleolar RNA host gene 1 aggravated prostate cancer development by sponging miR-377-3p to upregulate protein kinase B (AKT2). The results of miRNA microarrays uncovered that miR-377 expression was reduced in chordoma samples [20]. In this study, we tested the interaction between miR-377-3p and LOC554202 and analyzed their functional correlation in chordoma development.

It is widely accepted that miRNAs can suppress the translational process or induce the degradation of target messenger RNAs (mRNAs) by interacting with their 3′ untranslated region (3′UTR) [21,22]. Previous studies have suggested that miR-377-3p could regulate cancer progression by interacting with diverse molecules, including HOXC6 [18], JAG1 [17], DCP1A [23] and AKT2 [19]. Through bioinformatics analysis, sekelsky mothers against d PP SMAD) family member 3 (SMAD3) was predicted as a candidate target of miR-377-3p. Previous studies have identified SMAD3 as an oncogene in chordoma. For instance, Yao *et al*. [24] claimed that miR-149-3p overexpression hampered chordoma progression by downregulating SMAD3. Zhang *et al*. [25] found that miR-16-5p hampered the proliferation and metastasis of chordoma cells by downregulating SMAD3. Here, the interaction between miR-377-3p and SMAD3 was tested in chordoma cells and their functional correlation was explored.

We analyzed the expression pattern of LOC554202 in chordoma tissue samples and cell lines. Subsequently, loss-of-function experiments were conducted to assess the biological role of LOC554202 in chordoma cells. The downstream targets of LOC554202 were explored to illustrate its working mechanism in chordoma, which also provided potential targets for chordoma therapy.

Materials and methods

Clinical tissue samples

Nucleus pulposus samples ($n=29$) and skull-base chordoma samples ($n=29$) were collected from patients with disc herniation and chordoma patients at The Affiliated Nanhua Hospital, Hengyang Medical College, University of South China. This study was approved by the Research Ethics Committee of The Affiliated Nanhua Hospital, Hengyang Medical College, University of South China. None of these chordoma patients had received chemotherapy or radiotherapy before surgical resection. All the participants had signed the written informed consent before surgical resection.

Nucleus pulposus cell isolation and culture

Nucleus pulposus cells were isolated from patients with disc herniation as previously reported [26].

Three chordoma cell lines, including U-CH2, JHC7 and U-CH1 were purchased from BeNa Culture Collection (Beijing, China). All the cell lines were cultured with Iscove's Modified Dulbecco's modified Eagle's medium (Gibco, Grand Island, New York, USA) and Roswell Park Memorial Institute-1640 medium (Gibco) at the ratio of 4:1 plus 10% fetal bovine serum (FBS; Gibco), 1% 100 units/mL penicillin (Gibco) and 1% 100 μg/mL streptomycin (Gibco).

Quantitative real-time PCR

To analyze the expression of LOC554202 and SMAD3, cDNA was synthesized from RNA using the Bio-Rad iScript kit (Bio-Rad, Hercules, California, USA) followed by quantitative real-time PCR (qRT-PCR) using iQSYBR Green SuperMix (Bio-Rad). Glyceraldehyde-3-phosphate dehydrogenase (GAPDH) acted as the housekeeping gene. To measure the expression of miR-377-3p, reverse transcription was conducted using the TaqMan reverse transcription kit (Applied Biosystems, Rotkreuz, Switzerland) and qRT-PCR was conducted using the TaqMan MicroRNA assay kit (Applied Biosystems). U6 acted as the housekeeping gene. All primer sequences are shown in Table 1. The fold changes were analyzed by the $2^{-\Delta\Delta Ct}$ method.

Subcellular fractionation

Cytoplasmic or nuclear RNA was isolated using the PARIS Kit Protein and RNA Isolation System (Thermo Fisher Scientific, Waltham, Massachusetts, USA) according to the manufacturer's instructions. U6 or GAPDH was used as nuclear or cytoplasmic marker, respectively.

Cell transfection

LOC554202-specific small interfering (si)RNA (si-LOC554202), siRNA of E-cadherin (si-E-cadherin), siRNA of N-cadherin (si-N-cadherin), negative control of siRNA (si-NC), LOC554202 specific short hairpin (sh) RNA (sh-LOC554202), sh-NC, LOC554202 expressing plasmid (LOC554202), SMAD3 expressing plasmid (SMAD3), pcDNA empty vector (vector), miR-377-3p,

Table 1 Primers used in qRT-PCR

Gene	Direction	Sequence
LOC554202	Forward	5′-TCTCTGGTGCTTCCCTCCTT-3′
	Reverse	5′-GATCTAAGCTTGAGCCCCCA-3′
miR-377-3p	Forward	5′-TCGGCAGGATCACACAAAGGCA-3′
	Reverse	5′-CTCAACTGGTGTCGTGGA-3′
SMAD3	Forward	5′-GGGGTAATTTATTGCCGCCG-3′
	Reverse	5′-GAATGTCGCATCCTGTGGGA-3′
U6	Forward	5′-CTCGCTTCGGCAGCACA-3′
	Reverse	5′-AACGCTTCACGAATTTGCGT-3′
GAPDH	Forward	5′-GACAGTCAGCCGCATCTTCT-3′
	Reverse	5′-GCGCCCAATACGACCAAATC-3′

miR-NC, specific inhibitor of miR-377-3p (anti-miR-377-3p) and negative control (anti-miR-NC) were purchased from GenePharma (Shanghai, China). RNA or plasmid was transfected into chordoma cells with Lipofectamine 3000 (Invitrogen, Carlsbad, California, USA).

3-(4, 5-dimethylthiazol-2-yl)-2, 5 diphenyltetrazolium bromide assay

Transfected chordoma cells were seeded onto the 96-well plates. A commercial 3-(4, 5-dimethylthiazol-2-yl)-2, 5 diphenyltetrazolium bromide (MTT) kit (Sigma, Louis, Missouri, USA) was used to analyze the proliferation of chordoma cells. A total of 20 µL 5 mg/mL MTT reagent was added to the wells to incubate with chordoma cells for 4 h at 37 °C. The absorbance at 490 nm was determined.

Colony formation assay

Chordoma cells were seeded onto 6-well plates at the density of 150 cells/well. After incubation for 14 days, the culture supernatant was discarded and the colonies were washed with PBS (Sangon Biotech, Shanghai, China) three times. The colonies were fixed and then dyed with 0.1% crystal violet (Sangon biotech). After discarding the crystal violet solution, the colonies were washed and air-dried. The number of colonies was manually counted.

Flow cytometry

Cell apoptosis rate was analyzed using a commercial Annexin V-fluorescein isothiocyanate (FITC)/propidium iodide (PI) kit (Beyotime, Shanghai, China). After transfection for 72 h, chordoma cells were collected and incubated with Annexin V-FITC and PI for 30 min in the darkroom at room temperature. Cell fluorescence was measured on the Influx Flow Cytometer & Cell Sorter System (BD Biosciences, Franklin Lakes, New Jersey, USA). The apoptosis rate (the percentage of cells with $FITC^+$ and $PI^{+/-}$) was analyzed.

Transwell assays

The 24-well transwell chamber with 8 µM pore (Costar, Corning, New York, USA) precoated with Matrigel (BD Biosciences; in transwell invasion assay) or not (in transwell migration assay) was used in this study. After transfection for 24 h, chordoma cells in medium without serum were added to upper chambers, and 10% FBS was used as a chemokine in lower chambers. After incubation for 24 h in a cell incubator, migrated or invaded chordoma cells in the lower surface of the membrane were stained using 0.1% crystal violet (Sangon biotech) for 15 min. Stained cells at the magnification of 100 were photographed and then counted.

Wound healing assay

A wound healing assay was performed to assess cell migration ability. Transfected chordoma cells were seeded into 6-well plates. When cell confluence reached about 95%, the cell surface was scraped using a 200 µL pipette tip. Cell debris was removed through washing three times using PBS (Sangon Biotech). Cell images were obtained at the magnification of 40 after creating the wound for 0 h and 24 h.

Western blot assay

Transfected chordoma cells were disrupted using cell lysis buffer (Beyotime). Proteins were loaded onto an SDS-PAGE gel and blotted on the polyvinylidene difluoride (PVDF) membrane (Millipore, Billerica, Massachusetts, USA). The membrane was blocked using 5% skimmed milk for 1 h, and the membrane was then labeled with primary antibodies at 4 °C overnight. The membrane was mixed with horseradish peroxidase (HRP)-conjugated secondary antibody (Abcam, Cambridge, Massachusetts, USA). Protein blots were appeared by using the enhanced chemiluminescence (ECL) kit (GE Healthcare, Chicago, Illinois, USA). All primary antibodies were acquired from Abcam, including anti-E-cadherin (ab231303), anti-N-cadherin (ab207608), anti-SMAD3 (ab52903) and anti-GAPDH (ab181602).

Xenograft tumor analysis

A total of 16 BALB/c male nude mice (4-week-old) were purchased from Vital River Laboratory Animal Technology (Beijing, China) and were maintained in a pathogen-free environment at 22 ± 2 °C with 60% humidity under 12 h light/dark cycle. U-CH1 cell line stably transfected with sh-LOC554202 or sh-NC was established. A total of 1×10^6 U-CH1 cells suspended in 200 µL PBS buffer were subcutaneously injected into the right forelimb of the nude mice ($n = 8$/group). After injection for 8 days, tumor volume was calculated every 3 days as $\text{width}^2 \times \text{length} \times 0.5$. After injection for 23 days, all nude mice were euthanized by CO_2 asphyxia, and xenograft tumors were resected and weighed. Tumor tissues were used for qRT-PCR, H&E staining and immunohistochemistry assays. The animal experiment was approved by the Animal Care and Use Committee of The Affiliated Nanhua Hospital, Hengyang Medical College, University of South China.

Immunohistochemistry assay

To assess the expression of proliferation-related protein (Ki67), apoptosis-related proteins (BAX, BAK, BIM, BCL-2, BCL-XL and MCL1) and metastasis-associated protein (MMP9) in tumor tissues, immunohistochemistry assay was conducted with the following antibodies as previously reported [27]. Anti-Ki67 (ab245113), anti-BAX (ab32503), anti-BAK (ab32371), anti-BIM (ab32158), anti-BCL-2 (ab32124), anti-BCL-XL (ab32370), anti-MCL1 (ab32087) and anti-MMP9 (ab76003) were purchased from Abcam.

Bioinformatics prediction

The miRNA targets of LOC554202 were predicted by the LncBase database (http://carolina.imis.

athena-innovation.gr/diana_tools/web/index.php?r=lncbasev2%2Findex), whereas the mRNA targets of miR-377-3p were predicted by the TargetScan database (http://www.targetscan.org).

Dual-luciferase reporter assay

The fragment of LOC554202 or SMAD3, harboring the wild-type (WT) binding sequence with miR-377-3p, was amplified and constructed into luciferase reporter vector pmirGLO vector (Promega, Madison, Wisconsin, USA), termed as WT-LOC554202 or SMAD3 3′UTR-WT. Meanwhile, a matching mutant-type (MUT) fragment was also inserted into the pmirGLO vector (Promega), termed as MUT-LOC554202 or SMAD3 3′UTR-MUT. Afterward, chordoma cells were transfected with miR-NC or miR-377-3p and WT-LOC554202, MUT-LOC554202, SMAD3 3′UTR-WT or SMAD3 3′UTR-MUT. Luciferase activities were measured via the Dual-Luciferase Reporter Assay Kit (Promega).

RNA immunoprecipitation assay

RNA immunoprecipitation (RIP) assay was performed with Magna RIP RNA-Binding Protein Immunoprecipitation Kit (Millipore). Cell lysate was incubated with sepharose beads (Bio-Rad) that precoated with the antibody of Argonaute-2 (Ago2; Bio-Rad) or Immunoglobulin G (IgG; Bio-Rad). qRT-PCR was used for examination of LOC554202, miR-377-3p and SMAD3 levels.

Detection of glucose uptake, lactate production and ATP/ADP ratios

The consumption of glucose and the production of lactate in the culture supernatant were analyzed using Glucose Assay Kit (Abcam) and Lactic Acid Kit (Abcam) in accordance with the manufacturer's instructions. The relative ATP/ADP ratios were determined using ApoSENSOR ADP/ATP Ratio Assay Kit (BioVision, Milpitas, California, USA) in accordance with the manufacturer's instructions.

Statistical analysis

Results were shown as mean ± SD. Each experiment was conducted three times with at least three technical replicates. Statistical significance was assessed using Student's *t*-test for two groups and one-way analysis of variance (ANOVA) followed by Tukey's test in multiple groups. Linear correlation was analyzed using the Pearson correlation coefficient. A value of $P < 0.05$ was identified as statistically significant.

Results

LOC554202 expression is elevated in chordoma

The expression of LOC554202 was measured in 29 chordoma tissues and 29 nucleus pulposus tissues by qRT-PCR. LOC554202 was markedly upregulated in chordoma tissues compared with nucleus pulposus tissues (Fig. 1a). The LOC554202 level was also found to be notably elevated in three chordoma cell lines compared with nucleus pulposus cells (Fig. 1b). We analyzed the subcellular distribution of LOC554202 in chordoma cells. We found that LOC554202 was mainly distributed in the cytoplasmic fraction of chordoma cells (Fig. 1c,d), suggesting that LOC554202 function in chordoma cells at the post-transcriptional level. These data suggested that LOC554202 might be implicated in chordoma progression.

LOC554202 knockdown restrains the proliferation, migration and invasion and induces the apoptosis of chordoma cells

qRT-PCR verified the knockdown efficiency of si-LOC554202 and the overexpression efficiency of LOC554202 expressing plasmid in chordoma cells (Fig. 2a). Then, loss-of-function experiments were conducted to analyze the biological role of LOC554202 in chordoma cells. Cell proliferation ability was analyzed by MTT and colony formation assays. We found that LOC554202 knockdown significantly suppressed the proliferation ability of chordoma cells (Fig. 2b). The number of colonies was also reduced by silencing LOC554202 (Fig. 2c). Flow cytometry was performed to analyze the apoptosis rate of chordoma cells via Annexin V-FITC/PI double staining. As shown in Fig. 2d, LOC554202 knockdown significantly elevated the apoptosis rate of chordoma cells. LOC554202 knockdown reduced the number of migratory chordoma cells (Fig. 2e), suggesting that LOC554202 silencing suppressed the migration ability of chordoma cells. As mentioned in Fig. 2f, LOC554202 knockdown decreased the number of invasive chordoma cells, demonstrating that LOC554202 knockdown inhibited the invasion ability of chordoma cells. The width of the wound was significantly reduced in the si-NC group after 24-h incubation compared with the si-LOC554202 group (Fig. 2g), suggesting that LOC554202 interference suppressed cell migration in chordoma cells. E-cadherin and N-cadherin are two key molecules in the epithelial-to-mesenchymal transition (EMT) of cancer cells. During cancer progression, epithelial tumor cells may undergo EMT, a morphological and functional remodeling, that profoundly changes the characteristics of tumor cells, resulting in the loss of epithelial markers such as E-cadherin, changes in cell polarity and intercellular junctions and the increase of mesenchymal markers (N-cadherin, fibronectin and vimentin). We measured the expression of E-cadherin and N-cadherin in LOC554202-silenced chordoma cells. As shown in Fig. 2h,i, LOC554202 knockdown increased the protein expression of E-cadherin and reduced the protein level of N-cadherin. Taken together, we found that LOC554202 played a pro-tumor function to facilitate

Fig. 1

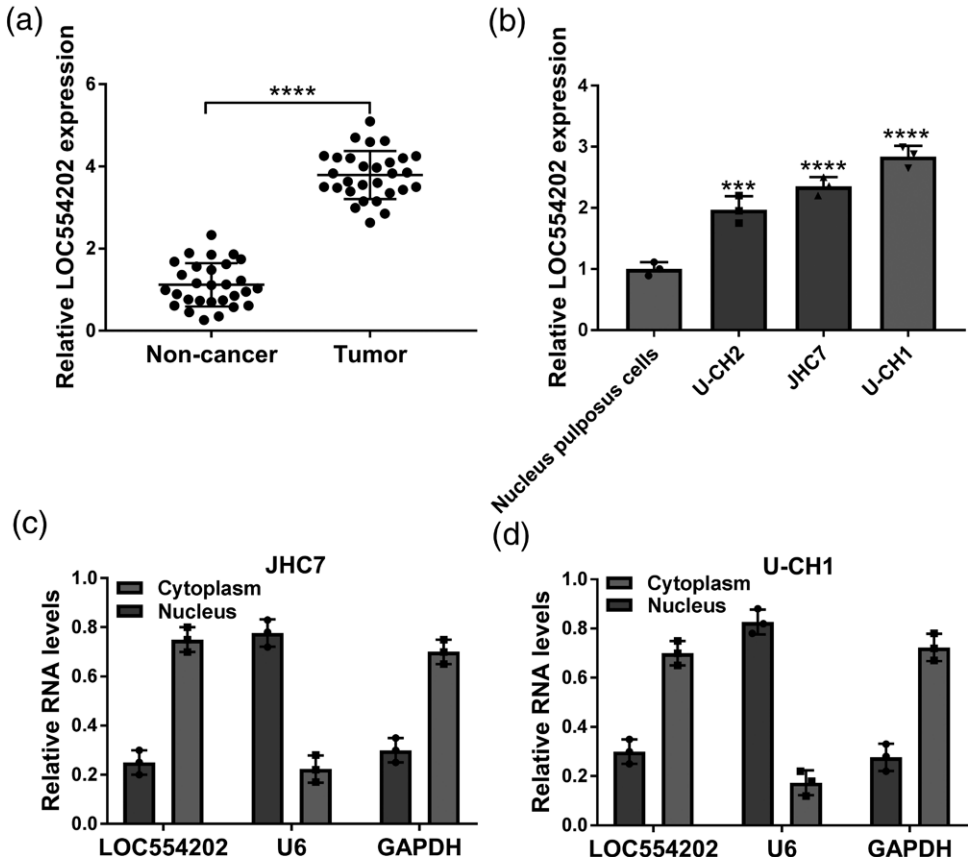

LOC554202 expression is elevated in chordoma. (a) qRT-PCR was applied to measure the expression of LOC554202 in tissues of nucleus pulposus ($n=29$) and chordoma ($n=29$). (b) The level of LOC554202 in three chordoma cell lines (U-CH2, JHC7 and U-CH1) and nucleus pulposus cells was determined by qRT-PCR. (c,d) Subcellular distribution of LOC554202 in JHC7 and U-CH1 cells was analyzed. U6 and GAPDH were used as nuclear marker and cytoplasmic marker due to their extensive distribution in nucleus and cytoplasm, respectively. ***$P<0.001$, ****$P<0.0001$. GAPDH, glyceraldehyde-3-phosphate dehydrogenase; qRT-PCR, quantitative real-time PCR.

the proliferation, migration and invasion and suppress the apoptosis of chordoma cells.

Considering that LOC554202 could regulate the migration and invasion abilities of chordoma cells, and LOC554202 could also regulate the protein levels of E-cadherin and N-cadherin, we proposed the hypothesis that LOC554202 functioned by regulating E-cadherin and N-cadherin expression. We silenced E-cadherin and N-cadherin in chordoma cells and analyzed cell proliferation, migration and invasion abilities. Western blot assay verified the knockdown efficiencies of si-N-cadherin and si-E-cadherin in chordoma cells (Supplementary Figure 1A and 1B, Supplemental digital content 1, http://links.lww.com/ACD/A441). We found that the knockdown of N-cadherin or E-cadherin had almost no effect on the proliferation of chordoma cells (Supplementary Figure 1C and 1D, Supplemental digital content 1, http://links.lww.com/ACD/A441). Meanwhile, the results showed that the knockdown of N-cadherin significantly suppressed the migration and invasion abilities of chordoma cells, whereas E-cadherin knockdown caused the opposite effects (Supplementary Figure 1E–1G, Supplemental digital content 1, http://links.lww.com/ACD/A441). These results suggested that LOC554202 could regulate the metastasis of chordoma cells by regulating the expression of E-cadherin and N-cadherin.

LOC554202 interference suppresses tumorigenesis of xenograft tumors *in vivo*

We established a xenograft tumor model to explore the role of LOC554202 in regulating tumor formation and growth *in vivo*. U-CH1 cell line stably transfected with sh-LOC554202 or sh-NC was established (Fig. 3a). The right forelimb of the nude mice was subcutaneously injected with U-CH1 cells stably transfected with sh-NC or sh-LOC554202. Tumor volume was measured every 3 days after injection for 8 days to draw a tumor growth curve. LOC554202 silencing significantly restrained the growth of xenograft tumors (Fig. 3b). After injection for 23 days, xenograft tumors were resected and weighed.

Fig. 2

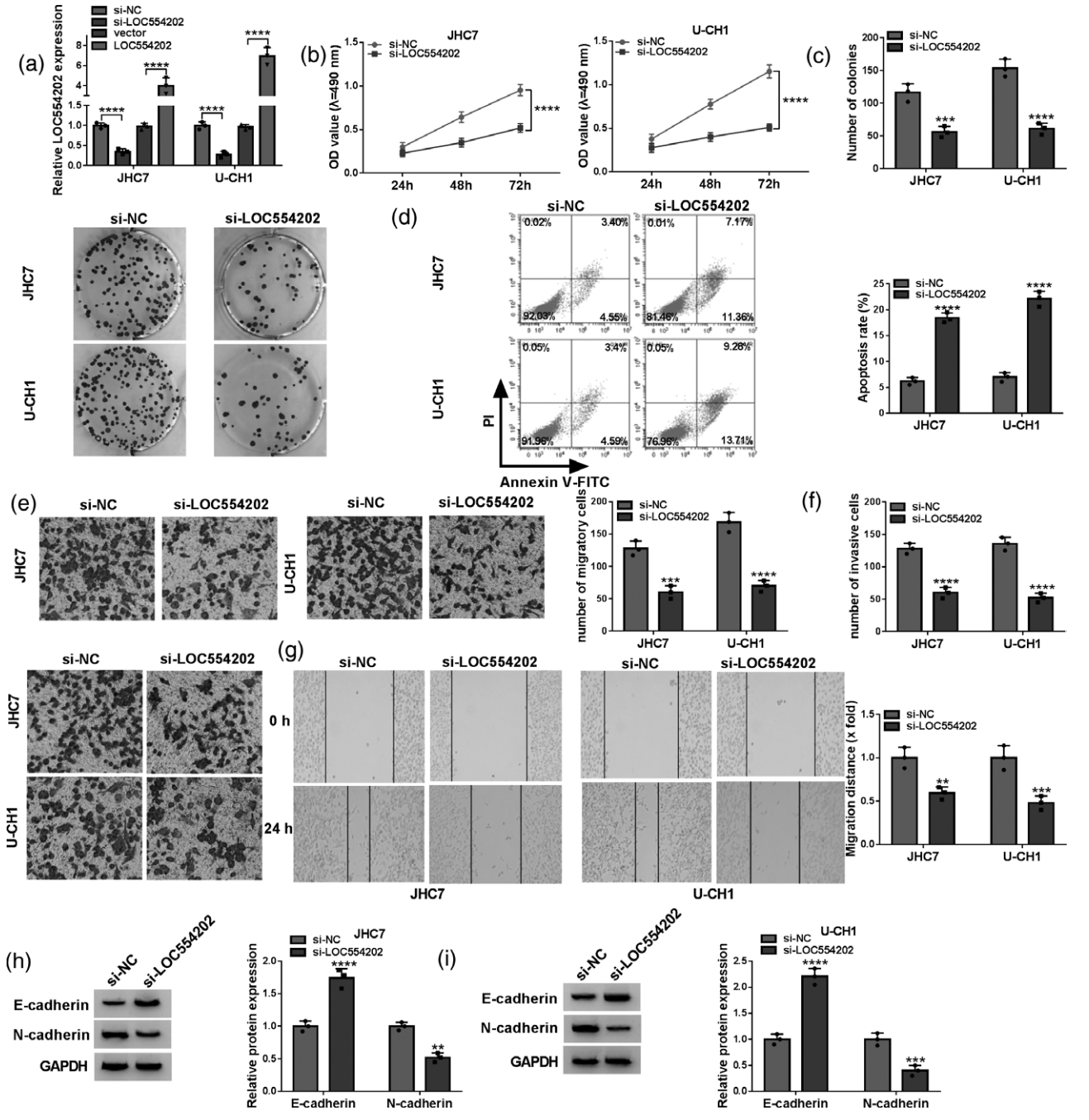

LOC554202 knockdown restrains cell proliferation, migration and invasion and induces cell apoptosis in chordoma cells. (a) The expression of LOC554202 in JHC7 and U-CH1 cells transfected with si-NC, si-LOC554202, vector or LOC554202 was determined by qRT-PCR. (b–i) JHC7 and U-CH1 cells were transfected with si-NC or si-LOC554202. (b) MTT assay was performed to assess the proliferation ability of chordoma cells. (c) Cell proliferation was analyzed by colony formation assay. The number of colonies was counted after incubation for 2 weeks. (d) Dot plot showed the Annexin V-FITC/PI staining of chordoma cells after transfection for 72 h. (e) The number of migratory chordoma cells was analyzed by transwell migration assay. (f) Transwell invasion assay was conducted to assess the number of invasive chordoma cells. (g) Wound healing assay was performed to evaluate cell migration ability. (h,i) The expression of E-cadherin and N-cadherin was measured by western blot assay. $^{**}P<0.01$, $^{***}P<0.001$, $^{****}P<0.0001$. FITC/PI, annexin V-fluorescein isothiocyanate/propidium iodide; MTT, 3-(4, 5-dimethylthiazol-2-yl)-2, 5 diphenyltetrazolium bromide; qRT-PCR, quantitative real-time PCR.

We found that LOC554202 interference notably reduced tumor weight compared with that in the sh-NC group (Fig. 3c). The expression of LOC554202 was notably decreased in the sh-LOC554202 group than that in the

sh-NC group (Fig. 3d), suggesting the successful knockdown of LOC554202 *in vivo*. The levels of proliferation-related protein (Ki67), apoptosis-related proteins (BAX, BAK, BIM, BCL-2, BCL-XL and MCL1) and metastasis-associated protein (MMP9) in tumor tissues were determined by immunohistochemistry assay. As shown in Fig. 3e, the expression of Ki67, MMP9 and three antiapoptotic proteins (BCL-2, BCL-XL and MCL1) was reduced in the sh-LOC554202 group compared with that in the sh-NC group. Besides, the levels of three pro-apoptotic proteins (BAX, BAK and BIM) were upregulated in the sh-LOC554202 group than that in the sh-NC group (Fig. 3e). Taken together, LOC554202 knockdown notably restrained xenograft tumor growth *in vivo*.

miR-377-3p is a target of LOC554202 in chordoma cells

miR-377-3p was predicted as a candidate target of LOC554202 by the LncBase database, and their potential binding sites were shown in Fig. 4a. Subsequently, to verify the target relationship between miR-377-3p and LOC554202, a dual-luciferase reporter assay and RIP assay were performed. We constructed luciferase plasmid WT-LOC554202 that contained the wild-type fragment of LOC554202. WT-LOC554202 was co-transfected with miR-NC or miR-377-3p into JHC7 and U-CH1 cells. As shown in Fig. 4b,c, luciferase activity was dramatically reduced in miR-377-3p and WT-LOC554202 group compared with the miR-NC and WT-LOC554202 group, demonstrating the target relationship between miR-377-3p and LOC554202. Also, to verify the interacted sites between miR-377-3p and LOC554202, we mutated the predicted miR-377-3p-binding sites in LOC554202, and the mutant fragment of LOC554202 was also constructed to the luciferase vector to generate MUT-LOC554202. Luciferase activity remained unaffected in the MUT-LOC554202 group with the co-transfection of miR-NC or miR-377-3p, suggesting that miR-377-3p interacted with LOC554202 via the predicted binding sites. miR-377-3p and LOC554202 were both pulled down when using the Ago2 antibody (Fig. 4d,e), suggesting that miR-377-3p and LOC554202 were simultaneously existed in RNA-induced silencing complex (RISC). miR-377-3p expression was significantly decreased in chordoma tissues compared with nucleus pulposus tissues (Fig. 4f). The level of miR-377-3p was also reduced in chordoma cell lines than that in nucleus pulposus cells (Fig. 4g). Given the opposite tendency of miR-377-3p and LOC554202 expression, the Pearson correlation coefficient was used to analyze the linear correlation between miR-377-3p and LOC554202. The miR-377-3p level was negatively correlated with LOC554202 expression (Fig. 4h). The expression of miR-377-3p was elevated with the knockdown of LOC554202, and its expression was reduced after overexpressing LOC554202 in chordoma cells (Fig. 4i), suggesting the negative regulatory relationship between LOC554202 and miR-377-3p. Overall, LOC554202 interacted with miR-377-3p in chordoma cells.

LOC554202 silencing-mediated effects in chordoma cells are largely offset by the silencing of miR-377-3p

Given the results that LOC554202 silencing suppressed the malignant behaviors of chordoma cells and

Fig. 3

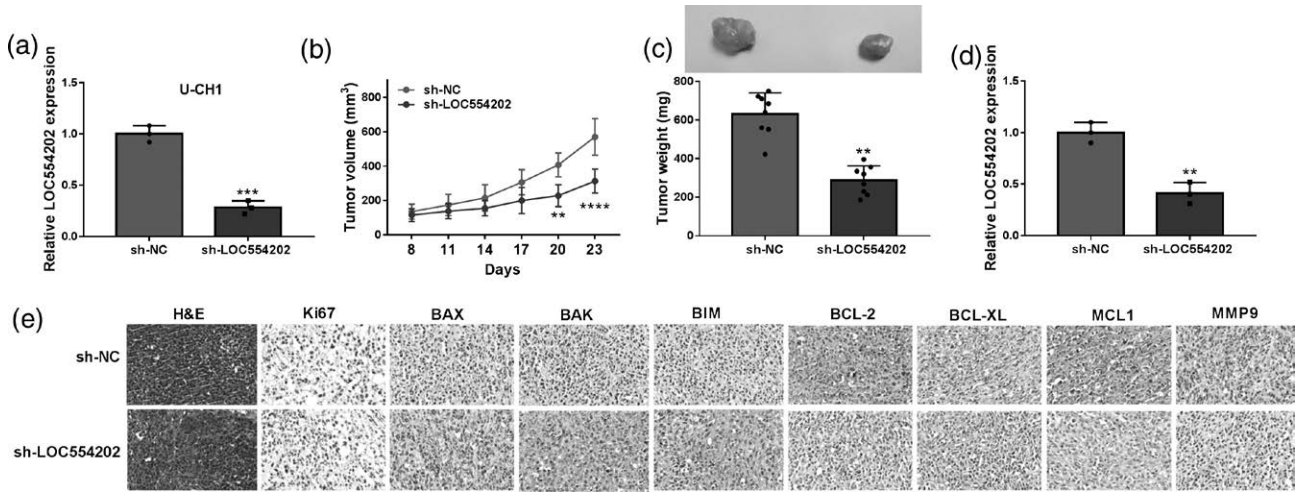

LOC554202 interference suppresses tumorigenesis of xenograft tumors *in vivo*. (a) qRT-PCR was used to verify if U-CH1 cell line stably expressing sh-LOC554202 was successfully established, and U-CH1 cell line stably expressing sh-NC was used as control. (b) Tumor volume was calculated every 3 days after injection for 8 days and growth curve was plotted. (c) Tumor weight was recorded after implantation for 23 days. (d) The expression of LOC554202 was examined in tumor tissues from two groups. (e) immunohistochemistry (IHC) assay was conducted to analyze the expression of Ki67, BAX, BAK, BIM, BCL-2, BCL-XL, MCL1 and MMP9 in tumor tissues. $^{**}P<0.01$, $^{***}P<0.001$, $^{****}P<0.0001$. qRT-PCR, quantitative real-time PCR.

Fig. 4

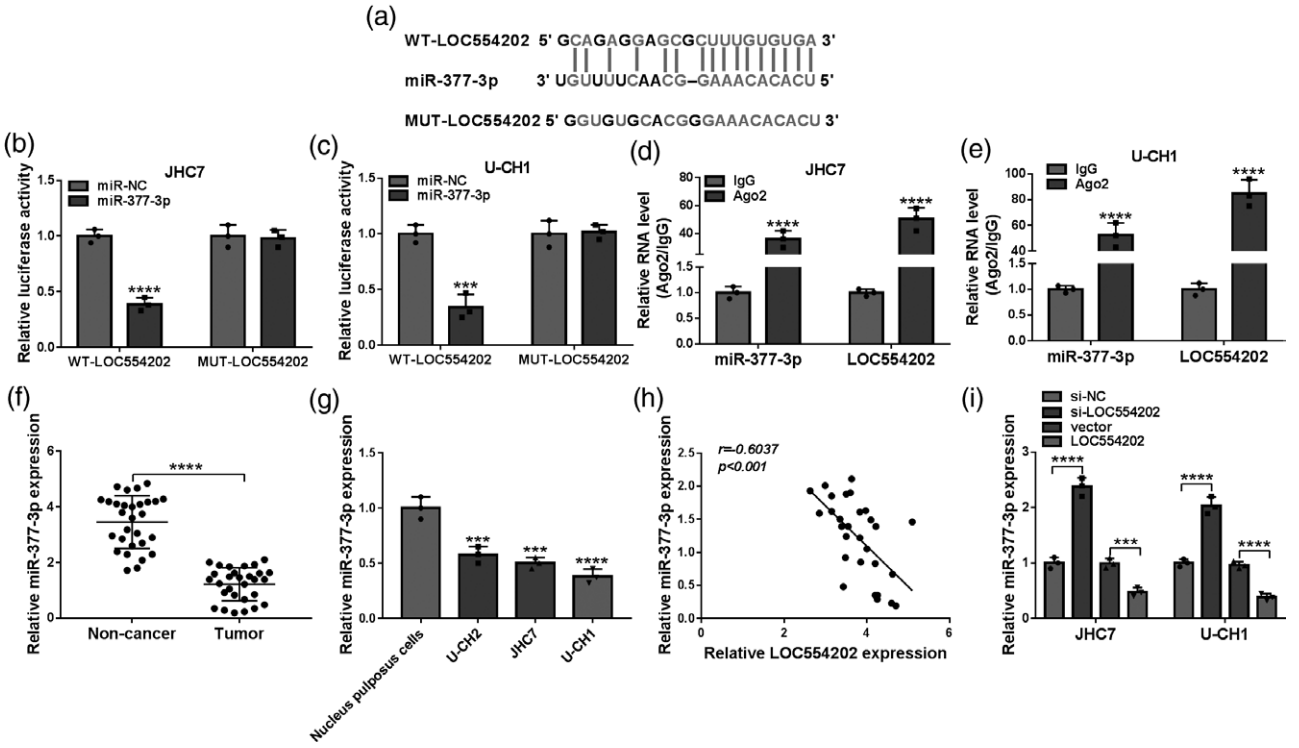

miR-377-3p is a target of LOC554202 in chordoma cells. (a) LncBase software was used to conduct bioinformatics analysis to predict the miRNA targets of LOC554202, and the potential binding sites between LOC554202 and miR-377-3p were shown. (b,c) Dual-luciferase reporter assay was conducted to analyze the luciferase activities in JHC7 and U-CH1 cells co-transfected with miR-NC or miR-377-3p and WT-LOC554202 or MUT-LOC554202 to confirm the target interaction. (d,e) RIP assay was performed to verify the interaction between miR-377-3p and LOC554202. (f) The expression of miR-377-3p was determined in nucleus pulposus tissues ($n=29$) and chordoma tissues ($n=29$) via qRT-PCR. (g) qRT-PCR was applied to analyze the expression of miR-377-3p in nucleus pulposus cells and a panel of chordoma cells. (h) Through analyzing the expression of miR-377-3p and LOC554202 in chordoma tissues, linear correlation between miR-377-3p and LOC554202 was generated via Pearson correlation coefficient. (i) The expression of miR-377-3p was determined in JHC7 and U-CH1 cells transfected with si-NC, si-LOC554202, vector or LOC554202 by qRT-PCR. ***$P<0.001$, ****$P<0.0001$. qRT-PCR, quantitative real-time PCR; RIP, RNA immunoprecipitation.

miR-377-3p was a target of LOC554202, we aimed to investigate if si-LOC554202-mediated effects could be alleviated by the silencing of miR-377-3p in chordoma cells. miR-377-3p expression was upregulated with the silencing of LOC554202, and the addition of anti-miR-377-3p reduced its expression again (Fig. 5a). The results of the MTT assay and colony formation assay demonstrated that miR-377-3p interference largely counteracted the inhibitory effect caused by LOC554202 knockdown on the proliferation of chordoma cells (Fig. 5b–d). LOC554202 silencing-mediated apoptosis in chordoma cells was also largely offset by the addition of anti-miR-377-3p (Fig. 5e). The migration ability in chordoma cells was largely recovered in si-LOC554202 and anti-miR-377-3p co-transfected group (Fig. 5f). Also, the results of the wound healing assay demonstrated that LOC554202 interference-induced suppression in cell migration ability was partly attenuated by the addition of anti-miR-377-3p (Fig. 5h). According to the results shown in Fig. 5g, the addition of anti-miR-377-3p regained cell invasion ability in LOC554202-silenced chordoma cells. LOC554202 interference-mediated upregulation in E-cadherin expression and reduction in N-cadherin expression were both alleviated by the addition of anti-miR-377-3p (Fig. 5i,j). These findings together demonstrated that LOC554202 silencing suppressed chordoma progression partly through upregulating miR-377-3p *in vitro*.

SMAD3 is a target of miR-377-3p in chordoma cells

TargetScan database was used to predict the downstream targets of miR-377-3p, and SMAD3 was predicted as one of the possible targets of miR-377-3p (Fig. 6a). The luciferase activity of WT reporter plasmid (SMAD3 3′UTR-WT) was notably reduced by miR-377-3p overexpression (Fig. 6b,c), suggesting the direct interaction between miR-377-3p and SMAD3 in chordoma cells. The results of the RIP assay revealed that SMAD3 existed in RISC, possibly through the binding relationship with miR-377-3p (Fig. 6d,e). SMAD3 mRNA and protein expression was upregulated in chordoma tissues compared with that in nucleus pulposus

Fig. 5

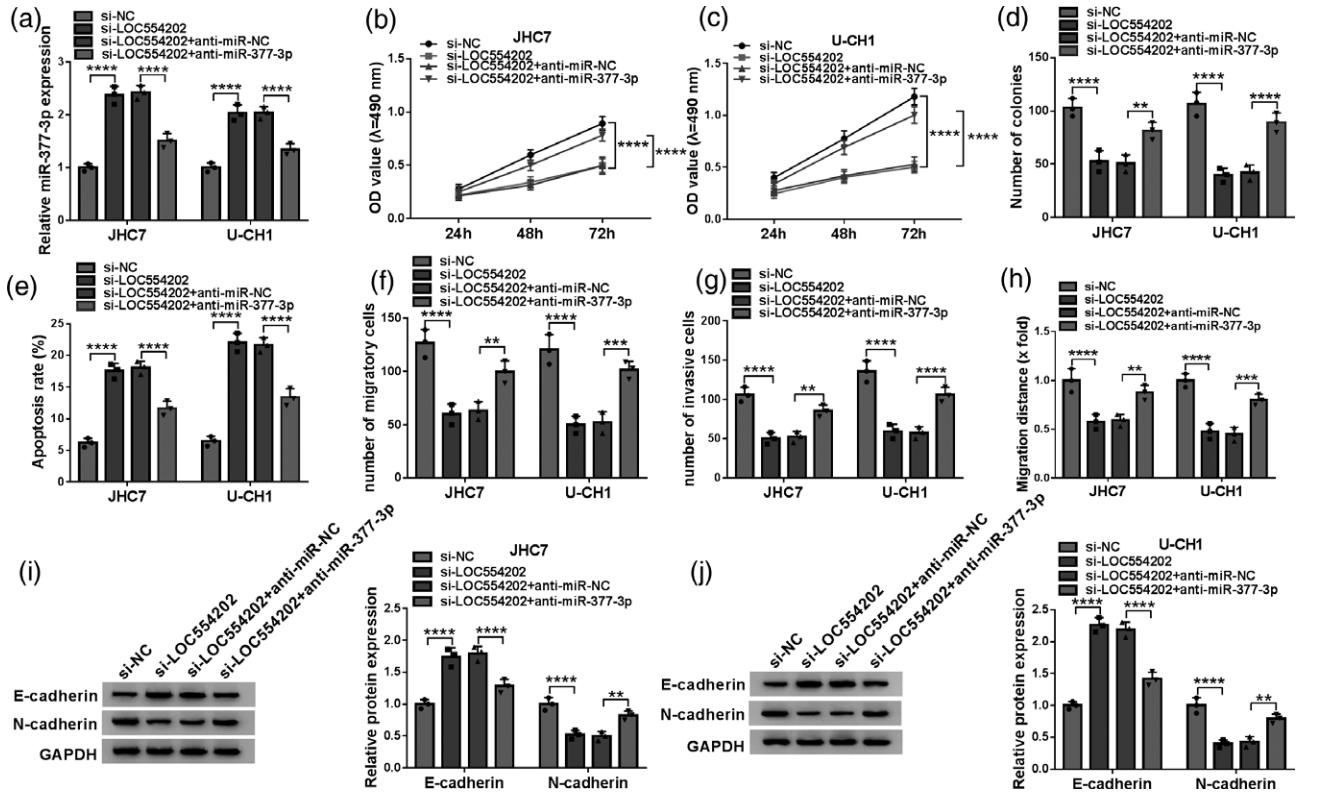

LOC554202 silencing-mediated effects in chordoma cells are largely offset by the silencing of miR-377-3p. (a–j) JHC7 and U-CH1 cells were transfected with si-LOC554202 alone or together with anti-miR-377-3p. (a) The expression of miR-377-3p was examined in chordoma cells by qRT-PCR. (b,c) Cell proliferation curve was drawn via MTT assay. (d) Colony formation assay was performed to evaluate cell proliferation ability. (e) Flow cytometry was conducted to analyze the apoptosis rate of chordoma cells. (f,g) Transwell migration and invasion assays were conducted to analyze the migration and invasion abilities of chordoma cells. (h) Cell migration ability was assessed by wound healing assay. (i,j) Western blot assay was applied for examination of protein levels of E-cadherin and N-cadherin. $^{**}P<0.01$, $^{***}P<0.001$, $^{****}P<0.0001$. MTT, 3-(4, 5-dimethylthiazol-2-yl)-2, 5 diphenyltetrazolium bromide; qRT-PCR, quantitative real-time PCR.

tissues (Fig. 6f,g). Compared with nucleus pulposus cells, SMAD3 protein expression was notably elevated in chordoma cells (Fig. 6h). There was a negative correlation between the expression of miR-377-3p and SMAD3 mRNA (Fig. 6i). The overexpression and interference efficiencies of miR-377-3p and anti-miR-377-3p were high in chordoma cells as confirmed by qRT-PCR (Fig. 6j). miR-377-3p overexpression reduced the protein expression of SMAD3 in chordoma cells (Fig. 6k). On the contrary, miR-377-3p silencing upregulated the protein level of SMAD3 in chordoma cells (Fig. 6k), suggesting that miR-377-3p negatively regulated SMAD3 expression in chordoma cells. These findings suggested that miR-377-3p interacted with the 3′UTR of SMAD3 in chordoma cells.

SMAD3 overexpression largely attenuates miR-377-3p-induced influences in chordoma cells

Given the negative regulatory relationship between miR-377-3p and SMAD3, we rescued the expression of SMAD3 through transfecting SMAD3 overexpression plasmid into miR-377-3p-overexpressed chordoma cells to conduct compensation experiments. As shown in Fig. 7a, SMAD3 protein expression was reduced with the overexpression of miR-377-3p, and the introduction of SMAD3 plasmid partly rescued the protein level of SMAD3 in JHC7 and U-CH1 cells. We found that miR-377-3p overexpression suppressed cell proliferation ability by conducting an MTT assay and colony formation assay (Fig. 7b–d). Cell apoptosis rate was significantly elevated with the overexpression of miR-377-3p (Fig. 7e). miR-377-3p overexpression was found to inhibit the migration ability in chordoma cells through analyzing the results of the transwell migration assay and wound healing assay (Fig. 7f,h). The number of invasive chordoma cells was reduced in the miR-377-3p-overexpressed group (Fig. 7g), suggesting that miR-377-3p overexpression suppressed cell invasion ability. miR-377-3p accumulation also caused a significant reduction in N-cadherin expression and upregulation in E-cadherin expression in chordoma cells (Fig. 7i,j). These results together further confirmed that

Fig. 6

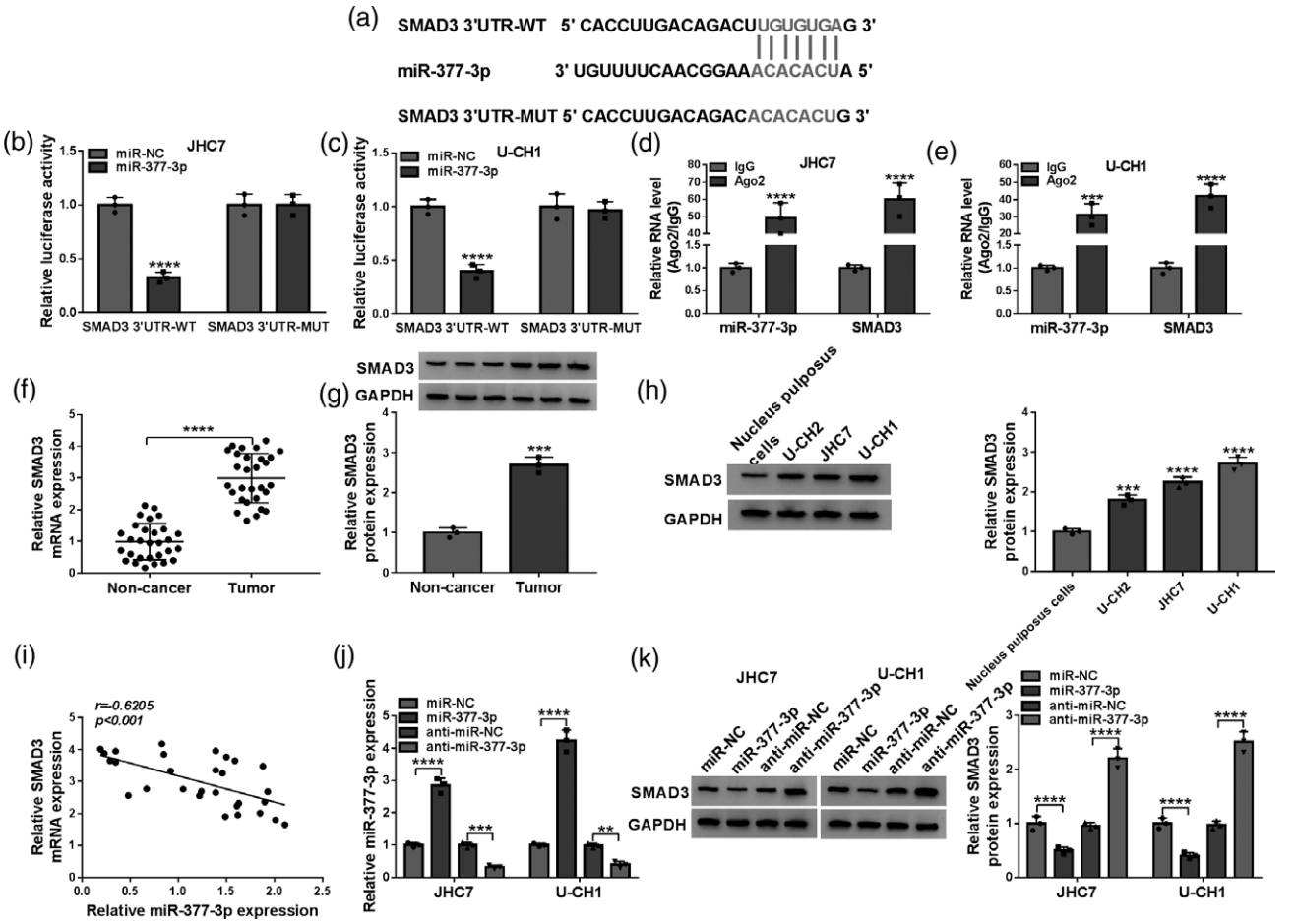

SMAD3 is a target of miR-377-3p in chordoma cells. (a) TargetScan bioinformatics database was used to seek the downstream targets of miR-377-3p, and the potential binding sequence between miR-377-3p and SMAD3 3′UTR was predicted. (b,c) JHC7 and U-CH1 cells were co-transfected with luciferase plasmids and miR-NC or miR-377-3p. Dual-luciferase reporter assay was applied to verify the target interaction between miR-377-3p and SMAD3. (d,e) The target interaction between miR-377-3p and SMAD3 was verified by RIP assay. (f,g) The mRNA and protein expression of SMAD3 in chordoma tissues and nucleus pulposus tissues was examined by qRT-PCR and western blot assay. (h) The protein level of SMAD3 in nucleus pulposus cells, U-CH2, JHC7 and U-CH1 cells was measured by western blot assay. (i) Pearson correlation coefficient was used to assess the linear relationship between the expression of miR-377-3p and SMAD3. (j,k) The expression of miR-377-3p and SMAD3 was determined in JHC7 and U-CH1 cells transfected with miR-NC, miR-377-3p, anti-miR-NC or anti-miR-377-3p via qRT-PCR and western blot assay. $^{**}P<0.01$, $^{***}P<0.001$, $^{****}P<0.0001$. qRT-PCR, quantitative real-time PCR; RIP, RNA immunoprecipitation; UTR,untranslated region.

miR-377-3p exerted an antitumor role in chordoma. The addition of SMAD3 plasmid largely recovered the proliferation ability in chordoma cells (Fig. 7b–d). miR-377-3p-induced apoptosis was largely suppressed by the addition of the SMAD3 plasmid (Fig. 7e). SMAD3 plasmid co-transfection in miR-377-3p-overexpressed chordoma cells also recovered the migration and invasion abilities in chordoma cells (Fig. 7f–h). SMAD3 overexpression reduced the expression of E-cadherin while elevated the level of N-cadherin in chordoma cells (Fig. 7i,j). Overall, miR-377-3p overexpression suppressed the proliferation, migration and invasion and promoted the apoptosis of chordoma cells partly through targeting SMAD3.

LOC554202 sponges miR-377-3p to up-regulate SMAD3 in chordoma cells

JHC7 and U-CH1 cells were transfected with si-LOC554202 alone or together with anti-miR-377-3p. LOC554202 silencing reduced the protein expression of SMAD3 in chordoma cells, which was largely rescued by silencing miR-377-3p (Fig. 8a,b), demonstrating that LOC554202 could positively regulate SMAD3 expression by sponging miR-377-3p in chordoma cells.

Cancer cells uptake glucose and transform it into lactate under aerobic condition, which is also known as the Warburg effect [28]. Warburg effect not only provides cancer cells energy for survival, proliferation and metastasis, but it also minimizes the production of reactive oxygen

Fig. 7

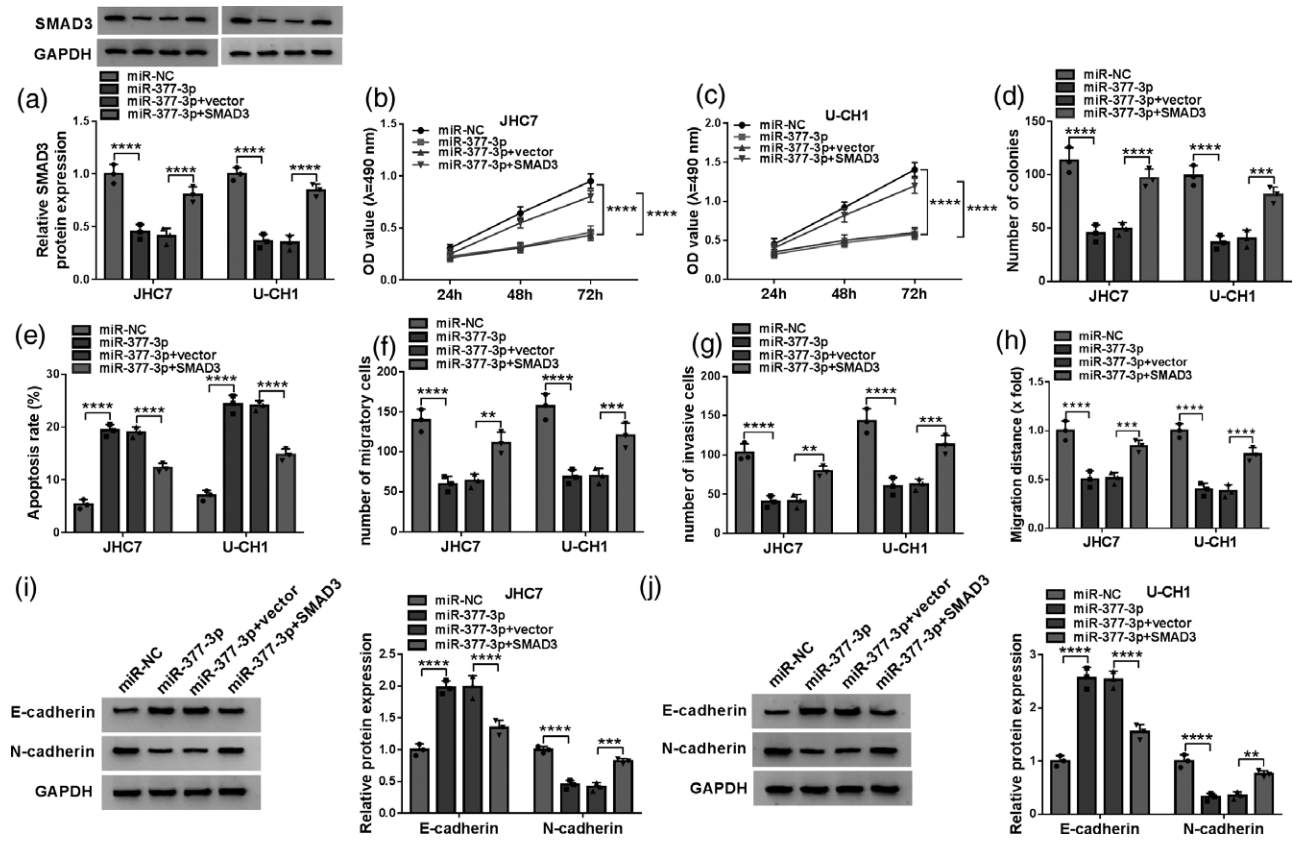

SMAD3 overexpression largely attenuates miR-377-3p-induced influences in chordoma cells. (a–j) JHC7 and U-CH1 cells were transfected with miR-NC, miR-377-3p, miR-377-3p + vector or miR-377-3p + SAMD3. (a) Western blot assay was utilized to measure the protein level of SMAD3 in chordoma cells. (b,c) Cell growth curve was plotted through estimating the number of chordoma cells after transfection for 24, 48 or 72 h. (d) Cell proliferation ability was assessed through analyzing the number of colonies after 2-week incubation. (e) Flow cytometry was used to evaluate the apoptosis rate in chordoma cells after transfection for 72 h. (f,g) The numbers of migratory and invasive chordoma cells were measured by transwell migration and invasion assays. (h) Wound healing assay was used to analyze migratory distance to evaluate cell migratory ability. (i,j) The levels of E-cadherin and N-cadherin were measured by western blot assay. $^{**}P<0.01$, $^{***}P<0.001$, $^{****}P<0.0001$.

species in mitochondria, thus offering a growth advantage for tumors [29,30]. We analyzed the role of LOC554202/miR-377-3p/SMAD3 on the glycolysis of chordoma cells, and the data showed that LOC554202 knockdown suppressed the uptake of glucose and the production of lactate and reduced the ratio of ATP/ADP in chordoma cells, which were largely reversed by miR-377-3p knockdown or SMAD3 overexpression (Fig. 9a–c). These data showed that LOC554202 facilitated the glycolysis of chordoma cells by mediating miR-377-3p/SMAD3 axis.

Discussion

LncRNAs are found to be widely dysregulated in many malignancies, and dysregulated lncRNAs play an oncogenic or tumor suppressor role in human malignancies [31]. A previous work reported that LOC554202 expression was upregulated in cervical cancer, and a high LOC554202 level predicted a dismal prognosis of cervical cancer patients [32]. Lin *et al.* [33] claimed that LOC554202 expression was upregulated in gastric cancer, and it facilitated the proliferation and motility of gastric cancer cells by regulating p21 and E-cadherin. He *et al.* [34] demonstrated that LOC554202 elevated the gefitinib resistance of nonsmall cell lung cancer cells by targeting miR-31. Furthermore, the study by Ma *et al.* [12] claimed that LOC554202 contributed to chordoma progression by regulating EZH2 and miR-31. Consistent with the previous study [12], we found that the expression of LOC554202 was elevated in chordoma. Subsequently, loss-of-function experiments were conducted to analyze the biological role of LOC554202 in chordoma cells. LOC554202 silencing caused significant suppression in cell proliferation, migration and invasion and notable promotion in cell apoptosis, suggesting the oncogenic role of LOC554202 in chordoma cells.

Xenograft tumor analysis was conducted to verify the role of LOC554202 in the growth of xenograft tumors. LOC554202 silencing significantly suppressed tumor growth *in vivo*. More in-vivo studies about the function of LOC554202 in chordoma metastasis will be conducted in the future.

Fig. 8

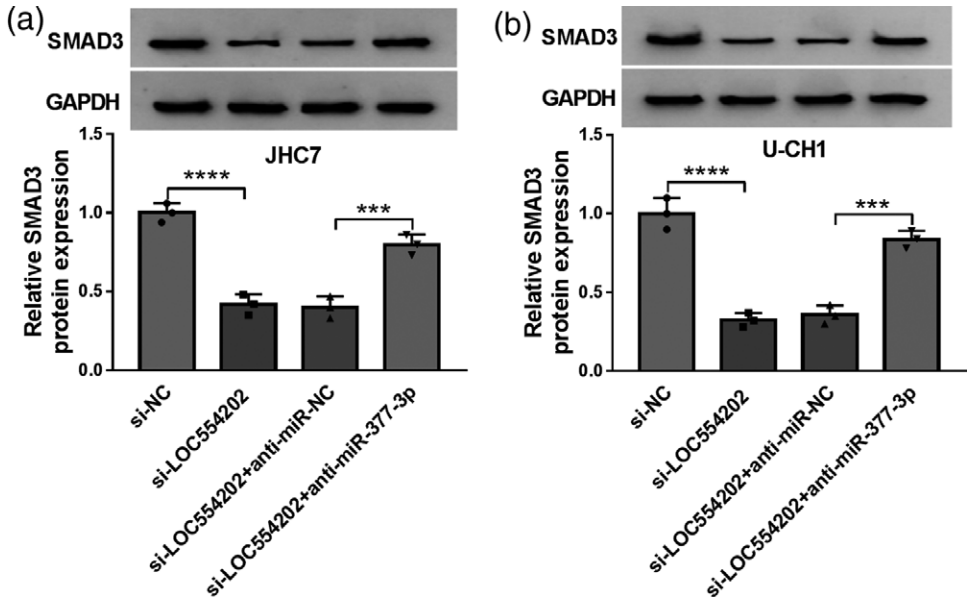

LOC554202 sponges miR-377-3p to upregulate SMAD3 in chordoma cells. (a,b) The protein level of SMAD3 was determined in chordoma cells transfected with si-NC, si-LOC554202, si-LOC554202 + anti-miR-NC or si-LOC554202 + anti-miR-377-3p via western blot assay. ***$P<0.001$, ****$P<0.0001$.

Fig. 9

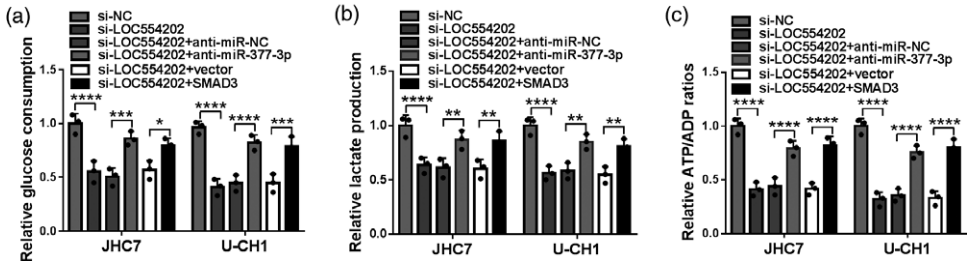

LOC554202 knockdown suppresses the glycolysis of chordoma cells through mediating miR-377-3p/SMAD3 axis. (a–c) JHC7 and U-CH1 cells were transfected with si-LOC554202 alone or together with anti-miR-377-3p or SMAD3 plasmid. The uptake of glucose, the production of lactate, and the relative ATP/ADP ratios were analyzed using glucose assay kit, lactic acid kit and ApoSENSOR ADP/ATP ratio assay kit, respectively. *$P<0.05$, **$P<0.01$, ***$P<0.001$, ****$P<0.0001$.

Subsequently, we aimed to seek the downstream targets of LOC554202, and the LncBase database was used to identify the possible interacted miRNAs of LOC554202. miR-377-3p was predicted as a target of LOC554202, and the interaction between LOC554202 and miR-377-3p was subsequently verified. miR-377-3p suppressed the development of several malignancies, including chordoma. Tang *et al*. [17] found that miR-377-3p hampered ovarian cancer development. miR-377-3p suppressed the development of prostate cancer by targeting AKT2 [19]. miR-377 expression was found to be decreased in chordoma tissues via miRNA microarrays [20]. We found that miR-377-3p expression was notably reduced in chordoma, which was in line with a previous study [20]. Besides, miR-377-3p level was negatively regulated by LOC554202 in chordoma cells. LOC554202 knockdown-mediated effects were largely counteracted by the silencing of miR-377-3p, suggesting that LOC554202 silencing suppressed the malignant progression of chordoma partly through upregulating miR-377-3p. Combined with the previous study by Ma *et al*. [12] we concluded that LOC554202 could contribute to the progression of chordoma by targeting multiple miRNAs, including miR-31 and miR-337-3p.

SMAD3 has been reported to exert a pro-tumor function in human malignancies. For example, SMAD3 facilitated the growth and motility in cervical cancer

cells [35]. Zhu *et al.* [36] found that melatonin suppressed the growth of gastric cancer via elevating the miR-16-5p level, thus reducing SMAD3 expression, suggesting the pro-proliferative role of SMAD3 in gastric cancer cells. In chordoma, SMAD3 was also found to contribute to the malignant behaviors of chordoma cells [24,25]. Zhang *et al.* [25] claimed that SMAD3 acted as the target of miR-16-5p to promote the proliferation and metastasis of chordoma cells. Yao *et al.* [24] found that SMAD3 was a target of miR-149-3p, and SMAD3 contributed to chordoma progression. SMAD3 was verified to bind to miR-377-3p, and the negative relationship between miR-377-3p and SMAD3 was found in chordoma cells. To explore if miR-377-3p functioned in chordoma cells by targeting SMAD3, we conducted rescue experiments by transfecting SMAD3 plasmid into miR-377-3p-overexpressed chordoma cells to rescue the expression of SMAD3. The results disclosed that miR-377-3p suppressed the malignant behaviors of chordoma cells through downregulating SMAD3. LOC554202 acted as miR-377-3p sponge to enhance SMAD3 level in chordoma cells. Interestingly, we found that LOC554202 could facilitate the glycolysis of chordoma cells by targeting miR-377-3p/SMAD3 axis.

In conclusion, our data suggested that LOC554202 was abnormally upregulated in chordoma. The interaction between miR-377-3p and LOC554202 or SMAD3 was identified in this study for the first time. LOC554202 facilitated the proliferation, migration, invasion and glycolysis and suppressed the apoptosis of chordoma cells by sponging miR-377-3p and upregulating SMAD3. LOC554202/miR-377-3p/SMAD3 axis may provide novel effective therapeutic targets for chordoma patients.

Acknowledgements

This study was supported by 2020 Scientific Research Plan Project of Hunan Provincial Health Commission [202104070680]; The Clinical Medical Technology Innovation Guidance Project of Hunan Technological Innovation Guidance Plan in 2017 [2017SK50221].

Conflicts of interest

There are no conflicts of interest.

References

1. Almefty K, Pravdenkova S, Colli BO, Al-Mefty O, Gokden M. Chordoma and chondrosarcoma: similar, but quite different, skull base tumors. *Cancer* 2007; **110**:2457–2467.
2. Gulluoglu S, Turksoy O, Kuskucu A, Ture U, Bayrak OF. The molecular aspects of chordoma. *Neurosurg Rev* 2016; **39**:185–196; discussion 196.
3. Patel P, Brooks C, Seneviratne A, Hess DA, Séguin CA. Investigating microenvironmental regulation of human chordoma cell behaviour. *PLoS One* 2014; **9**:e115909.
4. Gagliardi F, Boari N, Riva P, Mortini P. Current therapeutic options and novel molecular markers in skull base chordomas. *Neurosurg Rev* 2012; **35**:1–13; discussion 13.
5. Kayani B, Hanna SA, Sewell MD, Saifuddin A, Molloy S, Briggs TW. A review of the surgical management of sacral chordoma. *Eur J Surg Oncol* 2014; **40**:1412–1420.
6. Chugh R, Tawbi H, Lucas DR, Biermann JS, Schuetze SM, Baker LH. Chordoma: the nonsarcoma primary bone tumor. *Oncologist* 2007; **12**:1344–1350.
7. Yakkioui Y, van Overbeeke JJ, Santegoeds R, van Engeland M, Temel Y. Chordoma: the entity. *Biochim Biophys Acta* 2014; **1846**:655–669.
8. Peng WX, Koirala P, Mo YY. LncRNA-mediated regulation of cell signaling in cancer. *Oncogene* 2017; **36**:5661–5667.
9. Tsai MC, Spitale RC, Chang HY. Long intergenic noncoding RNAs: new links in cancer progression. *Cancer Res* 2011; **71**:3–7.
10. Ding J, Lu B, Wang J, Wang J, Shi Y, Lian Y, *et al.* Long non-coding RNA Loc554202 induces apoptosis in colorectal cancer cells via the caspase cleavage cascades. *J Exp Clin Cancer Res* 2015; **34**:100.
11. Shi Y, Lu J, Zhou J, Tan X, He Y, Ding J, *et al.* Long non-coding RNA Loc554202 regulates proliferation and migration in breast cancer cells. *Biochem Biophys Res Commun* 2014; **446**:448–453.
12. Ma X, Qi S, Duan Z, Liao H, Yang B, Wang W, *et al.* Long non-coding RNA LOC554202 modulates chordoma cell proliferation and invasion by recruiting EZH2 and regulating miR-31 expression. *Cell Prolif* 2017; **50**:e12388.
13. Di Leva G, Garofalo M, Croce CM. MicroRNAs in cancer. *Annu Rev Pathol* 2014; **9**:287–314.
14. Giordano S, Columbano A. MicroRNAs: new tools for diagnosis, prognosis, and therapy in hepatocellular carcinoma? *Hepatology* 2013; **57**:840–847.
15. Huang L, Liu Z, Hu J, Luo Z, Zhang C, Wang L, Wang Z. MiR-377-3p suppresses colorectal cancer through negative regulation on Wnt/β-catenin signaling by targeting XIAP and ZEB2. *Pharmacol Res* 2020; **156**:104774.
16. Jia M., Shi Y., Li Z., Lu X., Wang J. MicroRNA-146b-5p as an oncomiR promotes papillary thyroid carcinoma development by targeting CCDC6. *Cancer Lett* 2019; **443**:145–156.
17. Tang L, Yang B, Cao X, Li Q, Jiang L, Wang D. MicroRNA-377-3p inhibits growth and invasion through sponging JAG1 in ovarian cancer. *Genes Genomics* 2019; **41**:919–926.
18. Wang X, Chen T, Zhang Y, Zhang N, Li C, Li Y, *et al.* Long noncoding RNA Linc00339 promotes triple-negative breast cancer progression through miR-377-3p/HOXC6 signaling pathway. *J Cell Physiol* 2019; **234**:13303–13317.
19. Xie M, Zhang Z, Cui Y. Long noncoding RNA SNHG1 contributes to the promotion of prostate cancer cells through regulating miR-377-3p/AKT2 axis. *Cancer Biother Radiopharm* 2020; **35**:109–119.
20. Bayrak OF, Gulluoglu S, Aydemir E, Ture U, Acar H, Atalay B, *et al.* MicroRNA expression profiling reveals the potential function of microRNA-31 in chordomas. *J Neurooncol* 2013; **115**:143–151.
21. Ali Syeda Z, Langden SSS, Munkhzul C, Lee M, Song SJ. Regulatory mechanism of MicroRNA expression in cancer. *Int J Mol Sci* 2020; **21**:E1723.
22. Fabian MR, Sonenberg N, Filipowicz W. Regulation of mRNA translation and stability by microRNAs. *Annu Rev Biochem* 2010; **79**:351–379.
23. Shi C, Liu T, Chi J, Luo H, Wu Z, Xiong B, *et al.* LINC00339 promotes gastric cancer progression by elevating DCP1A expression via inhibiting miR-377-3p. *J Cell Physiol* 2019; **234**:23667–23674.
24. Yao J, Wu X. Upregulation of miR-149-3p suppresses spinal chordoma malignancy by targeting Smad3. *Onco Targets Ther* 2019; **12**:9987–9997.
25. Zhang H, Yang K, Ren T, Huang Y, Tang X, Guo W. miR-16-5p inhibits chordoma cell proliferation, invasion and metastasis by targeting Smad3. *Cell Death Dis* 2018; **9**:680.
26. Li W, Yao S, Li H, Meng Z, Sun X. Curcumin promotes functional recovery and inhibits neuronal apoptosis after spinal cord injury through the modulation of autophagy. *J Spinal Cord Med* 2021; **44**:1–9.
27. Liu H, Liu N, Cheng Y, Jin W, Zhang P, Wang X, *et al.* Hexokinase 2 (HK2), the tumor promoter in glioma, is downregulated by miR-218/Bmi1 pathway. *PLoS One* 2017; **12**:e0189353.
28. Warburg O. On the origin of cancer cells. *Science* 1956; **123**:309–314.
29. Liberti MV, Locasale JW. The Warburg Effect: How Does it Benefit Cancer Cells? *Trends Biochem Sci* 2016; **41**:211–218.
30. Vaupel P, Schmidberger H, Mayer A. The Warburg effect: essential part of metabolic reprogramming and central contributor to cancer progression. *Int J Radiat Biol* 2019; **95**:912–919.
31. Sanchez Calle A, Kawamura Y, Yamamoto Y, Takeshita F, Ochiya T. Emerging roles of long non-coding RNA in cancer. *Cancer Sci* 2018; **109**:2093–2100.
32. Chen J, Zhu J. Elevated expression levels of long non-coding RNA, Loc554202, are predictive of poor prognosis in cervical cancer. *Tohoku J Exp Med* 2017; **243**:165–172.

33. Lin Y, Zhang CS, Li SJ, Li Z, Sun FB. LncRNA LOC554202 promotes proliferation and migration of gastric cancer cells through regulating p21 and E-cadherin. *Eur Rev Med Pharmacol Sci* 2018; **22**:8690–8697.
34. He J, Jin S, Zhang W, Wu D, Li J, Xu J, Gao W. Long non-coding RNA LOC554202 promotes acquired gefitinib resistance in non-small cell lung cancer through upregulating miR-31 expression. *J Cancer* 2019; **10**:6003–6013.
35. Chang QQ, Chen CY, Chen Z, Chang S. LncRNA PVT1 promotes proliferation and invasion through enhancing Smad3 expression by sponging miR-140-5p in cervical cancer. *Radiol Oncol* 2019; **53**:443–452.
36. Zhu C, Huang Q, Zhu H. Melatonin inhibits the proliferation of gastric cancer cells through regulating the miR-16-5p-Smad3 pathway. *DNA Cell Biol* 2018; **37**:244–252.